

# A Low-profile 4-element Circularly Polarized Hexagonal DRA Array for Triple-band Wireless Applications

Anish Vahora<sup>1</sup>, Killol Pandya<sup>2</sup>

<sup>1,2</sup>Department of Electronics and Communication Engineering, Charotar University of Science and Technology, Changa, Gujarat, India.

Corresponding author: Anish Vahora (e-mail: anish.vahora@bvmengineering.ac.in)

**ABSTRACT** This paper presents a triple-band low-profile circularly polarized (CP) hexagonal dielectric resonator antenna (HDRA) array for various wireless applications. A 4-element linear array is designed using a simple microstrip power divider to improve the performance of the HDRA. This HDRA excites  $TE_{\delta 01}$  mode at a first resonant frequency of 1.52 GHz. The proposed design operates in three frequency bands, i.e. 1.44 - 1.61 GHz, 2.95 - 3.27 GHz, and 4.00 - 4.84 GHz with the fractional bandwidth of 10.98%, 11.02% and 22.20%, respectively. It also provides good gain and more than 70% of radiation efficiency with a better radiation pattern at all the resonating points. Further, it has a CP bandwidth of 50 MHz and 650 MHz around 3.12 GHz and 4.25 GHz, respectively. The proposed HDRA array is suitable for different wireless applications such as GPS (1 – 2 GHz), WiMAX (2 – 4 GHz), and WLAN (4 – 8 GHz).

**INDEX TERMS** Hexagonal DRA, Circularly polarization, Power divider, Tri-band, Wireless applications

## I. INTRODUCTION

The antennas are utilized as the front-end gadgets for the remote correspondence framework. However, it is getting progressively tricky to fulfilling the prerequisites such as miniaturized size, enhanced bandwidth, and performance for present-day innovations. This research gained interest in the wideband and multi-band systems that would support numerous wireless applications and printed antennas are preferred for such kinds of applications [1]. Particularly, microstrip patch antennas are used for many wireless communication applications due to the advanced features like low cost, ease to fabricate, and small size [1]. However, it has limitations like narrow bandwidth, low efficiency, and reduction in gain due to surface and metallic loss. Therefore, dielectric resonator antennas (DRAs) are used and offer the potential for upgraded performance for upcoming advancements with their attractive features [2-4]. Some of them are no surface waves, minimal conductor (ohmic) losses, and high radiation efficiency. DRAs gained interest due to their ability to provide wide bandwidth, enhanced gain characterizes by compact structure [5, 6]. The various shaped single element and array geometries are reported in the literature [7-21].

The modified rectangular shaped with microstrip line feed structure for the multi-band wireless application are proposed [7, 16, 20]. The three segments of RDRA gives a good level of isolation, but the resultant geometry becomes bulky. Therefore, different feeding techniques are used to get multi-band characteristics. Similarly, different shapes of DRA have also been used to generate multi-band features. Sharma et

al [8] presented a triple-band cylindrical DR antenna with filtering structure and parasitic slots are fed by an annular-shaped microstrip line. In order to make DR compact and for a slow-wave effect, two circular slots on the partial ground were introduced. Das et al [9] proposed a cylindrical dielectric resonator (Alumina Ceramic) and achieved 27% bandwidth with a 7.95 dB gain between 3.5 GHz and 4.75 GHz frequency band. A rectangular-shaped 4-element circularly polarized array is proposed by Rana et al [10] for microwave image sensing applications. The circular polarization has been achieved by exciting two orthogonal modes within the DRA. It has a maximum gain of 13.6 dBi with an axial ratio bandwidth of 10%. A novel compact bi-cone-shaped dielectric resonator antenna for ultra-wideband applications is presented by Sankaranarayanan et al [11]. The wider impedance bandwidth has been achieved due to the designed geometry increasing the surface area to volume ratio. Also, a hemispherical 4-element linear array is presented by Sarkar et al [12]. The designed array gives an impedance bandwidth of 7.2% with a gain of 10.7 dBi.

Altaf et al [13] proposed a triple-band dual-sense circularly polarized DRA for numerous wireless applications. A modified hexagonal DR has been top-loaded by a square microstrip ring (SMR) and fed by a vertical tapered strip connected to a 50 $\Omega$  microstrip line. The designed geometry resonates in different resonating bands with narrow fractional bandwidth. Cheh et al [14] presented a tri-band rectangular DRA with two ports using a hybrid technique that consists of a meander line antenna for LTE applications. Generally,

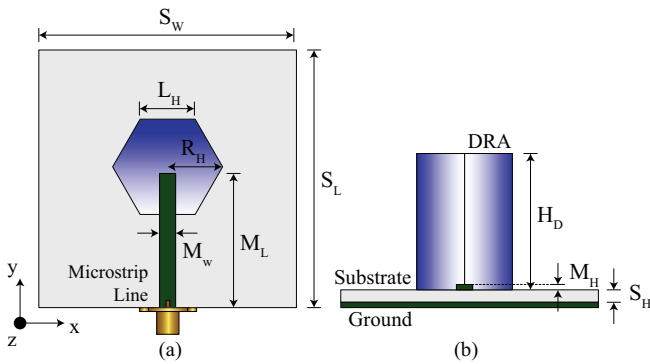


FIGURE 1: Conventional hexagonal DRA: (a) Top view (b) Perspective view.

TABLE 1: Detailed dimensions of the single HDRA

Symbol	$S_W$	$S_L$	$M_W$	$M_L$	$M_H$
Value [mm]	48.00	50.00	3.00	25.00	0.035
Symbol	$R_H$	$L_H$	$H_D$	$S_H$	–
Value [mm]	8.66	10.00	21.00	1.60	–

a rectangular shape is chosen because it provides one more degree of freedom than hemispherical DRAs and cylindrical DRAs [3]. A 4-element cylindrical-shaped DR array with beam steering is designed by Mishra et al [15]. The progressive phase shift has been achieved using an unequal feed network. Mukherjee et al [17] given a review of the recent advances in dielectric resonator antennas. The authors presented all types of DR geometries. Further, a 4-element cylindrical-shaped linear array is proposed for triple-band applications [18]. The designed array gives maximum bandwidth of 40%. Gupta et al [19] presented a circularly polarized stacked sapphire and TMM13i rectangular DRA for dual-band application. An aperture coupling type excitation has been used and gives an impedance bandwidth of 7.69%. Recently, Chauhan et al [21] reported the meta superstrate-based high gain and low profile circularly polarized DRA for wideband applications. Also, split-ring resonators are used to enhance the 3-dB axial ratio and impedance bandwidth of the geometry. The proposed single antenna and antenna arrays are provided good performance characteristics over the resonating bands. However, the implementation in the practical applications is challenging due to its size, and complex geometry. Therefore, in this work, the authors have proposed a simple hexagonal DRA array for various wireless applications.

In this paper, a 4-element low-profile hexagonal DRA is presented for triple-band wireless applications. The designed array gives circular polarization property at higher resonating bands. An unequal length microstrip power divider is designed in such a way as to excite the array at desired resonating bands. Also, partial ground plane topology has been used to improve the fractional bandwidth (FBW) of the structure. The designed array is placed on top of FR-4 low-cost substrate material. In simulation, the designed

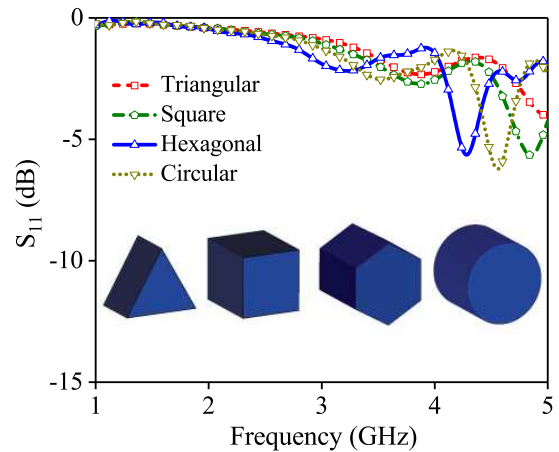


FIGURE 2: Effect on  $S_{11}$  magnitude with different shaped DRA.

array resonates at 1.52 GHz, 3.12 GHz, and 4.25 GHz with FBW of 11.00%, 10.30%, and 19.00%, respectively. Further, it provides good directivity and radiation efficiency over resonating bands. The simulated and measured results are perfectly matched. Therefore, the designed array structure is a perfectly suitable candidate for numerous wireless applications such as GPA/WiMAX/WLAN. The rest of the paper is organized as follows: The proposed single hexagonal DRA in Section II, and a 4-element linear array is given in Section III. Then, in Section IV, the parametric analysis and E-field distribution are described. Then, the simulated and measured results are given in Section V. Finally, Section VI presents the conclusion of the proposed work.

## II. PROPOSED SINGLE ELEMENT

Fig. 1 shows the proposed hexagonal DRA with a stripline feeding. Fig. 1(a) and (b) show the proposed geometry's top view and perspective view, respectively. In the above design, a substrate dimension of  $48 \times 50 \text{ mm}^2$ . Where material selected for DRA is alumina with a height of 21 mm and having relative permittivity,  $\epsilon_{dr} = 9.9$  and loss tangent  $\tan \delta = 0.0001$ . The partial ground approach has been used to improve the fractional bandwidth of the geometry, and it is shown in Fig. 1(b). Further, a low-cost FR-4 substrate material is used, with a dielectric permittivity of  $\epsilon_{sr} = 4.3$ , and the thickness of the substrate is 1.6 mm. The resonating frequency of the DRA can be calculated as follow. The proposed HDRA has been approximated to a rectangular DRA to find equivalent permittivity [13] ( $\epsilon_{eq}$ )

$$\epsilon_{eq} = \frac{\epsilon_{dr} \times V_{dr} + V_{air}}{V_{dr} + V_{air}} \quad (1)$$

where  $V_{air}$  and  $V_{dr}$  represent the volume of the air and dielectric resonator, respectively, and  $\epsilon_{dr}$  indicate the relative permittivity of the DR. With consideration of the relative permittivity of the substrate material, the overall resultant

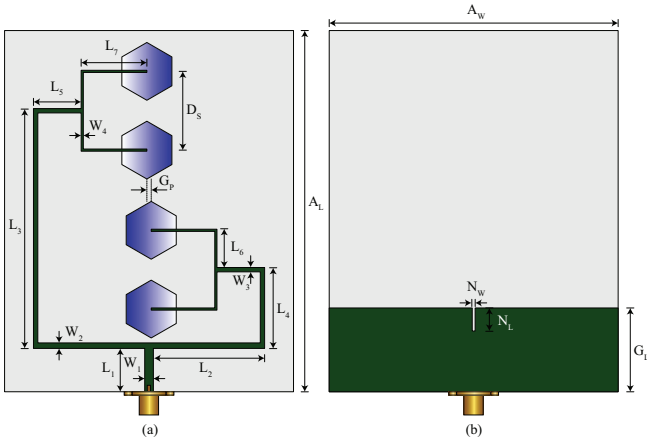


FIGURE 3: Proposed 4-element linear hexagonal DRA array: (a) Top view (b) Back-view.

TABLE 2: Detailed dimensions of the proposed 4-element HDRA array

Symbol	$A_w$	$A_L$	$G_L$	$N_w$	$N_L$	$G_p$
Value [mm]	100.00	125.00	29.00	1.00	8.00	1.50
Symbol	$D_s$	$W_1$	$W_2$	$W_3$	$W_4$	$L_1$
Value [mm]	27.25	3.00	1.90	1.50	0.75	15.00
Symbol	$L_2$	$L_3$	$L_4$	$L_5$	$L_6$	$L_7$
Value [mm]	38.50	83.00	28.00	16.50	13.25	22.75

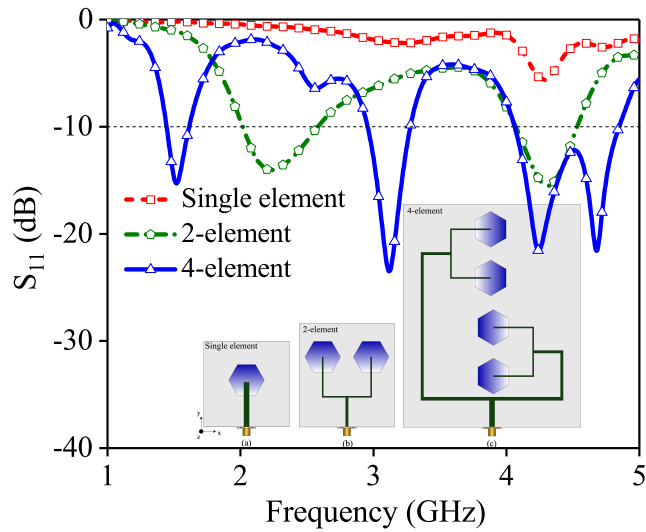


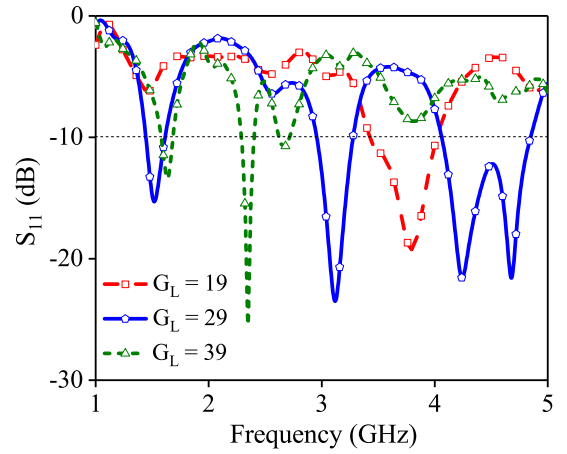
FIGURE 4: Reflection coefficient of single element, 2-element array, and 4-element array.

relative permittivity can be expressed as:

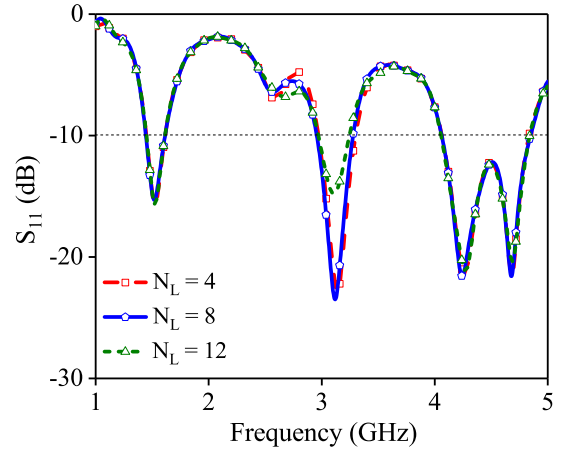
$$\epsilon_{re} = \frac{SD_H}{\frac{H_D}{\epsilon_{eq}} + \frac{S_H}{\epsilon_{sr}}} \quad (2)$$

where  $\epsilon_{sr}$  and  $S_H$  represent the relative permittivity and height of FR-4 substrate material, respectively, and where  $SD_H$  denotes the total height of the structure and is given as:

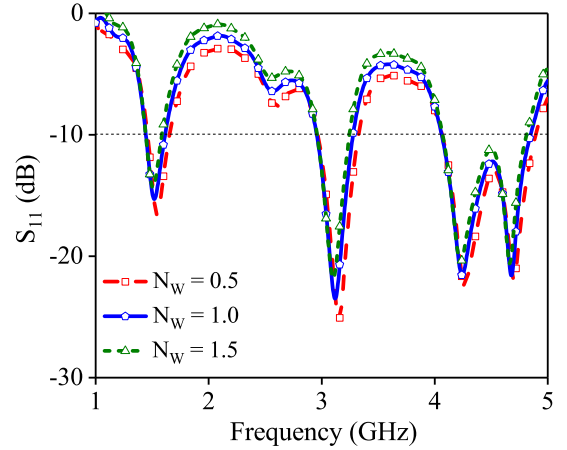
$$SD_H = H_D + S_H \quad (3)$$



(a)



(b)



(c)

FIGURE 5: Effect on  $S_{11}$ : (a) Ground length  $G_L$  variation (b) Back notch length  $N_L$  variation and (c) Back notch width  $N_w$  variation (unit:mm).

The resonance frequency ( $f_r$ ) of the DR structure has been calculated by

$$f_r = \frac{c}{2\pi\sqrt{\epsilon_{re}}} \sqrt{k_x^2 + k_y^2 + k_z^2} \quad (4)$$

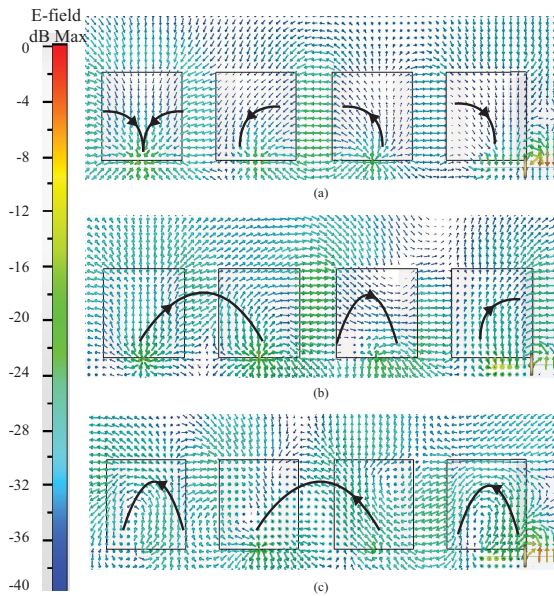


FIGURE 6: E-field distribution at: (a) 1.52 GHz (b) 3.12 GHz and (c) 4.25 GHz.

where  $k_x$ ,  $k_y$ , and  $k_z$  are expressed as  $\pi/\text{length}$  of DRA,  $\pi/\text{width}$  of DRA, and  $\pi/2 \times \text{height}$  of DRA, respectively. The detailed optimized dimensions of the proposed HDRA are given in Table 1. Hexagonal geometry is derived from cylindrical DR structures. Parameters like the dimensions of single-layer substrate and height of the DR with permittivity are given in Fig. 1. Mathematically, hexagonal DRA (HDRA) is obtained by connecting six equilateral triangles side by side, each of them having a side length ( $L_H$ ) of 10 mm, as shown in Fig. 1(a) and is calculated by Equation (5).

$$L_H = 2R_H \sin 30^\circ \quad (5)$$

Further, the various shapes such as triangular, square, and circular-shaped conventional DR structures are designed and compared reflection coefficient with hexagonal shaped DR structure. The designed various-shaped DR structures as well as their corresponding reflection coefficient are depicted in Fig. 2. From Fig. 2, it can be seen that overall conventional shaped DR structures, the hexagonal shape gives a quite good reflection coefficient curve as compared to others. Inspired by the hexagonal geometry results, the authors designed a 4-element linear array for various applications.

### III. PROPOSED 4-ELEMENT LINEAR ARRAY

The proposed 4-element HDRA structure top-view and back-view are illustrated in Fig. 3(a) and (b), respectively. The designed conventional hexagonal elements are placed on the y-axis with inter-element space of  $D_S$ . The slight gap between  $2 \times 1$  array structure is  $G_P$ , which is due to adjusting the feed network. The uniform power divider has been designed with non-uniform length to excite the  $2 \times 1$  subarray. The overall size of the designed array is  $125 \times 100 \text{ mm}^2$ . From Fig. 3(b), it can be seen that the ground plane is partially etched and an

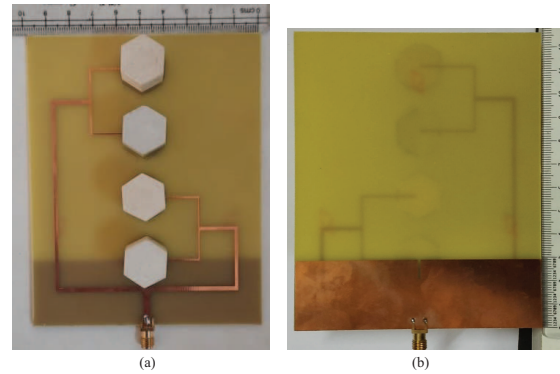


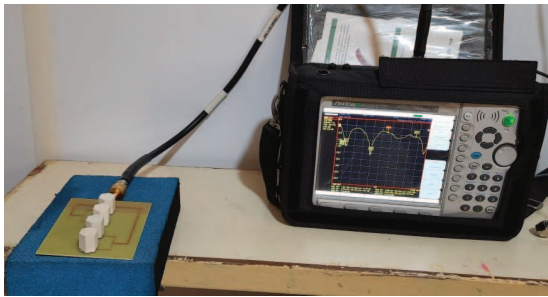
FIGURE 7: Proposed 4-element linear hexagonal DRA array: (a) Top-view (b) Back-view.

additional rectangular notch has been incorporated in at the center with a dimension of  $1 \times 8 \text{ mm}^2$ . It can be observed that the additional phased delay has been added to the feed line. The reason behind to introduced phased delay is to avoid the E-field cancellation. As  $2 \times 1$  array geometries are excited from the opposite side direction. Also, as compared to conventional feed network arrangement, the proposed feed network reduces overall size. The detailed dimensions of the proposed 4-element HDRA array are given in Table 2. All the dimensions are optimized in CST-MWS simulation software [22].

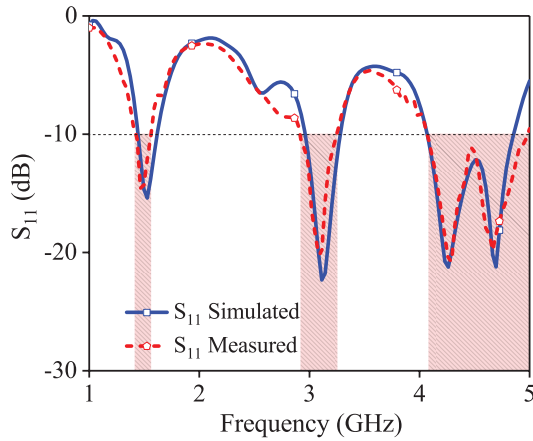
Further, the comparison between single element, 2-element array, and 4-element array in terms of reflection coefficient has been performed and depicted in Fig. 4. From Fig. 4 it can be observed that the proposed single element hexagonal geometry is not able to resonate at the desired band. While the 2-element linear array geometry gives dual-band characteristics with low impedance bandwidth. When the 4-element proposed linear array resonates at the desired frequency with good impedance bandwidth and returns loss. Further, the detailed study of the designed 4-element linear array is given in the next section.

### IV. PARAMETRIC AND E-FIELD ANALYSIS

The parametric analysis of the proposed structure, as well as E-field analysis, has been discussed in this section. There are various parameters such as length of the ground plane, notched width, and length which are responsible for the sharp resonance. The effect on  $S_{11}$  magnitude due to sensitive parameters is given in Fig. 5. The ground length  $G_L$  variation effect on reflection coefficient is depicted in Fig. 5(a). It can be observed that for a particular value the antenna resonates in the desired bands and gives a good performance. Similarly, the notch length and width variations are illustrated in Fig. 5(b) and (c), respectively. The parametric analysis has been carried out by varying separately by taking other parameter's optimized dimensions. Further, the simulated E-field distribution in the proposed geometry at 1.52 GHz, 3.12 GHz, and 4.25 GHz is given in Fig. 6(a), (b), and (c), respectively. The configuration exhibits fundamental mode



(a)



(b)

FIGURE 8: Simulated and measured reflection coefficient of proposed HDRA array: (a) Setup (b)  $S_{11}$  magnitude.



FIGURE 9: Anechoic chamber measurement setup.

$TE_{\delta 01}^x$  at 1.52 GHz and higher-order mode  $TE_{\delta 02}^x$  and  $TE_{\delta 03}^x$  at 3.12 GHz and 4.25 GHz, shown in Fig. 6(a)-(c).

### V. SIMULATION AND MEASUREMENT RESULTS

In this section, the designed array structure has been fabricated, tested, and compared with the state-of-the-art. In order to validate the design, the proposed 4-element HDRA array has been fabricated and tested in a laboratory. The fabricated prototype top-view and back-view are given in Fig. 7(a) and (b), respectively.

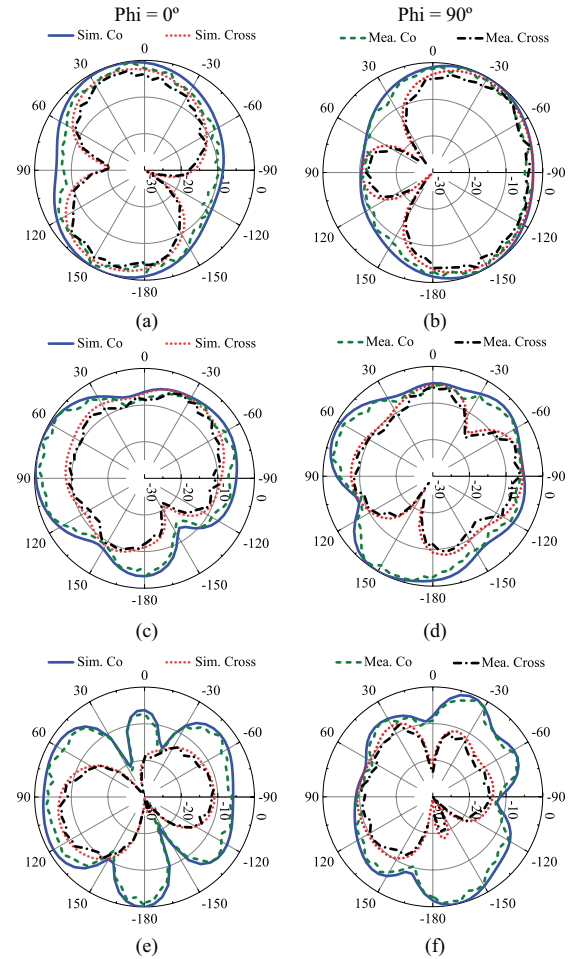


FIGURE 10: Simulated and measured 2D radiation patterns of the proposed array at: (a) 1.50 GHz (b) 3.10 GHz and (c) 4.20 GHz.

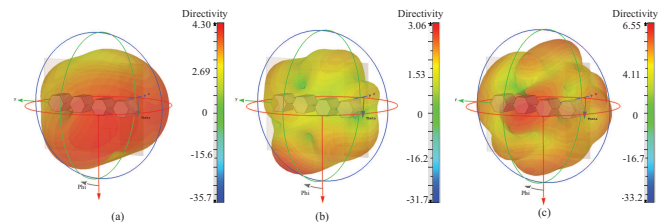


FIGURE 11: 3D directivity pattern of the proposed array at: (a) 1.52 GHz (b) 3.12 GHz and (c) 4.25 GHz.

### A. REFLECTION COEFFICIENT

The reflection coefficient measurement setup is illustrated in Fig. 8(a). It can be seen that the proposed HDRA array is connected to Vector Network Analyzer (VNA). The measured and simulated reflection coefficient of the proposed HDRA array is depicted in Fig. 8(b). It can be observed that the simulated and measured results are perfectly matched and give good performance. In measured results, the proposed array structure resonates at 1.50 GHz, 3.10 GHz, and 4.20 GHz with fractional impedance bandwidth of 10.98%, 11.02%,

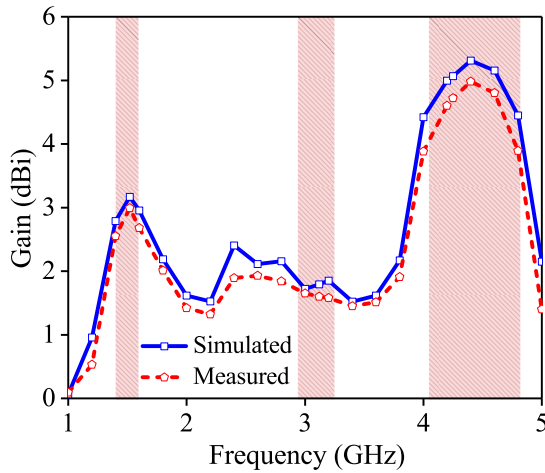


FIGURE 12: Simulated and measured gain of proposed HDRA array.

TABLE 3: Performance comparison of simulated and measured results

Parameters	Simulated			Measured		
	fr <sub>1</sub>	fr <sub>2</sub>	fr <sub>3</sub>	fr <sub>1</sub>	fr <sub>2</sub>	fr <sub>3</sub>
f <sub>r</sub> (GHz)	1.52	3.12	4.25	1.50	3.10	4.20
S <sub>11</sub> (dB)	-15.30	-23.50	-21.60	-14.70	-20.65	-21.30
FBW (%)	11.00	10.30	19.00	10.98	11.02	22.20
Gain (dBi)	3.17	2.01	5.08	3.10	1.95	4.97
Directivity (dBi)	3.97	2.43	6.46	–	–	–
Rad. Efficiency (%)	83.20	72.04	71.10	80.25	68.45	65.80
Axial Ratio (dB)	–	0.95	1.26	–	–	–
CP BW (MHz)	–	50	650	–	–	–

and 22.20%, respectively. Also, S<sub>11</sub> magnitude is less than -10 dB over the resonating bands.

**B. RADIATION PATTERNS**

The anechoic chamber has been used to perform the radiation pattern characteristics of the proposed antennas. The anechoic chamber measurement setup is given in Fig. 9. It can be seen that the proposed array SMA connector is connected with the turning table to measure both planes patterns. The 2D radiation patterns at 1.50 GHz, 3.10 GHz, and 4.20 GHz are given in Fig. 10(a)-(c). It can be noted that for all resonating frequencies, the proposed array gives a good radiation pattern. The difference between co and cross-pol is more than 20 dB which is due to the feed network. Also, it has a low sidelobe level which is more than -10 dB. Further, the sidelobe level can be improved to adjust the inter-element space. The simulated 3D directivity pattern at the resonating frequencies is given in Fig. 11. It can be noted that the directivity varies from 3.90 - 6.50 dBi over the resonating bands. Also, it has a maximum directivity of 6.46 dBi at 4.25 GHz.

**C. GAIN AND RADIATION EFFICIENCY**

The simulated and measured gain of the proposed array structure is depicted in Fig. 12. It can be noted that the measured gain varies from 1.80 - 5.01 dBi. The measured maximum gain of 4.97 dBi was achieved at 4.20 GHz. The

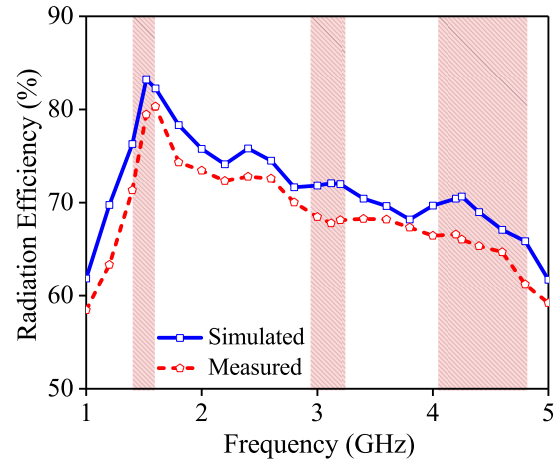


FIGURE 13: Simulated and measured radiation efficiency of proposed HDRA array.

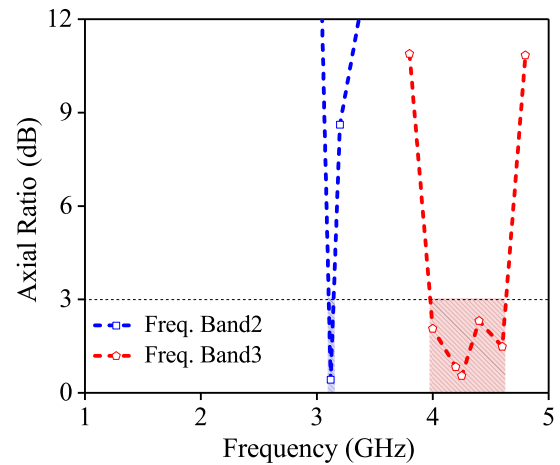


FIGURE 14: Simulated axial ratio of the proposed array geometry.

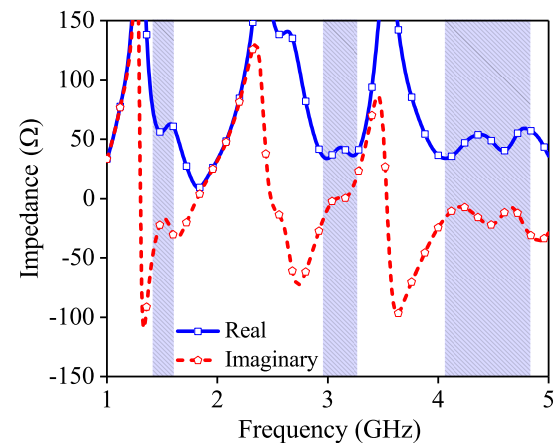


FIGURE 15: Proposed HDRA array impedance.

achieved gain over the resonating bands is quite acceptable for wireless applications. Also, the simulated and measured radiation efficiency of the proposed array geometry is given

TABLE 4: Comparison with the state-of-art DRAs

Ref.	DRA Shape	DRA material	Substrate	Type of feed	Size (mm) <sup>2</sup>	No. of bands	No. of element	Gain (dBi)	FBW (%)	Efficiency (%)
[7]	Rectangular	Plexiglass	FR-4	Microstrip line	41 × 25	3	1	3.5	3.4	---
[8]	Cylindrical	Alumina Ceramic	FR-4	Microstrip line	50 × 50	3	1	5.32	8.16	---
[9]	Cylindrical	Alumina Ceramic	FR-4	Annular shaped Microstrip line	115 × 80	1	4	7.95	27	---
[10]	Rectangular	Eccostock HIK	Arlon AD270	Microstrip line	135 × 48	1	4	13.6	17	92
[11]	Bi-cone	Rogers TMM10I	---	Coaxial probe	100 × 100	1	1	7.5	93.1	80
[12]	Hemispherical	Eccostock HIK	Arlon AD270	Microstrip line	135 × 48	1	4	10.7	7.5	---
[13]	Hexagonal	Alumina Ceramic	RF-35	Microstrip line	70 × 80	3	1	5.28	28.13	90
[14]	Rectangular	Eccostock HIK	FR-4	Microstrip line	90 × 50	3	1	4.1	18.93	80
[15]	Cylindrical	Rogers 3010	Rogers RT5870	Aperture Coupled	100 × 85	1	4	10	7	90
[16]	Rectangular	---	Rogers RT5880	Microstrip line	50 × 50	3	1	4	1.36	---
[18]	Cylindrical	Alumina Ceramic	FR-4	Microstrip line	120 × 120	3	4	9	40	73.36
[19]	Rectangular	Sapphire & TMM13i	FR-4	Aperture coupling	50 × 50	2	1	4.90	7.69	---
[20]	Rectangular	Alumina Ceramic	FR-4	Microstrip line	70 × 65	3	1	6.06	14	85
[21]	Cylindrical	Rogers RO3010	FR-4	Slot aperture	60 × 60	1	1	11.9	26.8	78
This work	Hexagonal	Alumina Ceramic	FR-4	Microstrip line	100 × 125	3	4	4.97	22.20	80.25

in Fig. 13. From Fig. 13 it can be noted that the radiation efficiency varies from 62.50 - 84.60% over the given frequency range. The measured maximum radiation efficiency of 80.25% was achieved at 1.50 GHz.

Further, the designed antenna array is circularly polarized at the higher modes. The axial ratio of the proposed array at around 3.10 GHz and 4.20 GHz is below 3 dB. The simulated axial ratio versus frequency plot is given in Fig. 14. It can be noted that the designed array geometry is circularly polarized and it has a circular polarization bandwidth of 50 MHz and 650 MHz, respectively. At the higher modes, circular polarization has been achieved due to the shape of the DRA and feeding network. Also, the impedance response of the array geometry is given in Fig. 15. It can be seen that an impedance is almost constant 50Ω in the resonating bands.

The designed array geometry simulated and measured performance parameters are given in Table 3. From Table 3, it can be observed that the simulated and measured results are exactly matched and minor variations in the resonating frequency and gain which is due to fabrication error, SMA connector, and material.

Further, the comparison of the proposed hexagonal DRA structure with state-of-the-art is given in Table 4. It can be observed that the designed array gives good performance in terms of fractional bandwidth as well as gain and radiation pattern. Therefore, the designed 4-element linear array structure is applicable for various wireless applications.

The authors find the major challenge is in the fabrication process of DRA. Also, the performance parameters could be improved by incorporating more elements in the array design. The Wilkinson power divider technique [23] could be utilized to design feeding network for the array.

## VI. CONCLUSION

The proposed circularly polarized 4-element hexagonal DRA is applicable for tri-band wireless applications. The proposed antenna array is excited with the help of a microstrip line, which generates TE<sub>δ01</sub> mode at 1.52 GHz. The dimensions of the proposed array are optimized using parametric analysis. The gain and fractional bandwidth are improved by incorporating the array and partial ground plane approach, respectively. The proposed array structure generates three different frequency bands, that is, 1.44 – 1.61 GHz, 2.95 – 3.27 GHz, and 4.00 – 4.84 GHz with the fractional bandwidth of 10.98%, 11.02%, and 22.20%, respectively. Also, it gives good gain, directivity, and good radiation efficiency. Further, it has a CP operating range of 3.10 – 3.15 GHz and 3.97 – 4.63 GHz. The proposed antenna design is suitable for GPS (L-band 1 – 2 GHz), WiMAX (S-band 2 – 4 GHz), and WLAN (C-band 4 – 8 GHz) applications.

## ACKNOWLEDGEMENT

The research was funded by Charotar University of Science and Technology (CHARUSAT) under the CHARUSAT Seed

Grant for research (Project No 14). The research was performed and carried out at Electronics and Communication Engineering department, Chandubhai S. Patel Institute of Technology, CHARUSAT University, Gujarat, India.

## REFERENCES

- [1] C. A. Balanis, *Antenna Theory: Analysis and Design*, Hoboken, NJ, USA: Wiley, 2016.
- [2] R. D. Richtmyer, "Dielectric resonator," *Journal of Applied Physics*, vol. 10, no. 6, pp. 391–398, 1939. doi:10.1063/1.1707320
- [3] A. Petosa, *Dielectric Resonator Antenna Handbook*, Norwood, MA, USA: Artech House, 2007.
- [4] K. W. Leung, E. H. Lim, and X. S. Fang XS, "Dielectric resonator antennas: From the basic to the aesthetic," *Proceedings of the IEEE*, vol. 100, no. 7, pp. 2181–2193, 2012. doi:10.1109/JPROC.2012.2187872
- [5] R. K. Mongia, and A. Ittipiboon, "Theoretical and experimental investigations on rectangular dielectric resonator antennas," *IEEE Transactions on antennas and propagation*, vol. 45, no. 9, pp. 1348–56, 1997. doi:10.1109/8.623123
- [6] R. K. Mongia, and P. Bhartia, "Dielectric resonator antennas - A review and general design relations for resonant frequency and bandwidth," *International Journal of Microwave and Millimeter-wave Computer-Aided Engineering*, vol. 4, no. 3, pp. 230–247, 1994. doi:10.1002/mmce.4570040304
- [7] M. Bemani, S. Nikmehr, and H. Younesiraad, "A novel small triple band rectangular dielectric resonator antenna for WLAN and WiMAX applications," *Journal of Electromagnetic Waves and Applications*, vol. 25, pp. 1688–1698, 2012. doi:10.1163/156939311797164864
- [8] A. Sharma, and R. K. Gangwar, "Compact tri-band cylindrical dielectric resonator antenna with circular slots," *Journal of Electromagnetic Waves and Applications*, vol. 30, no. 3, pp. 331–340, 2016. doi:10.1080/09205071.2015.1114430
- [9] G. Das, A. Sharma, and R. K. Gangwar, "Four element cylindrical dielectric resonator antenna array with annular shaped microstrip feed," *Antenna Test and Measurement Society (ATMS India-16)*, 2016.
- [10] B. Rana, and S. K. Parui, "Microstrip line fed wideband circularly-polarized dielectric resonator antenna array for microwave image sensing," *IEEE Sensors Letters*, vol. 1, no. 3, pp. 1–4, 2017. doi:10.1109/LESENS.2017.2696580
- [11] D. Sankaranarayanan, D. Venkatakiran, and B. Mukherjee, "Compact bi-cone dielectric resonator antenna for ultra-wideband applications-a novel geometry explored," *Electromagnetics*, vol. 37, no. 7, pp. 471–481, 2017. doi:10.1080/02726343.2017.1380257
- [12] G. A. Sarkar, B. Rana, and S. K. Parui, "A direct microstrip line feed hemispherical dielectric resonator antenna array," *2017 1st IEEE International Conference on Electronics, Materials Engineering and Nano-Technology (IEMENTech)*, 2017. doi:10.1109/IEMENTECH.2017.8076924
- [13] A. Altaf, and M. Seo, "Triple-Band Dual-Sense Circularly Polarized Hybrid Dielectric Resonator Antenna," *Sensors*, vol. 18, no. 11, p.3899, 2018. doi:10.3390/s18113899
- [14] I. K. Lin, M. H. Jamaluddin, A. Awang, R. Selvaraju, M. H. Dahri, L. C. Yen, H. A. Rahim, "A Triple Band Hybrid MIMO Rectangular Dielectric Resonator Antenna for LTE Applications," *IEEE Access*, vol. 7, pp. 122900–122913, 2019. doi:10.1109/ACCESS.2019.2937987
- [15] N. K. Mishra, S. Das, and D. K. Vishwakarma, "Beam steered linear array of cylindrical dielectric resonator antenna," *AEU-International Journal of Electronics and Communications*, vol. 98, pp. 106–113, 2019. doi:10.1016/j.aeue.2018.11.011
- [16] N. K. Darimireddy, C. W. Park, R. R. Reddy, and B. S. Reddy, "Multi-band rectangular hybrid antennas loaded with inter-digital structure slot," *In 2019 IEEE Indian Conference on Antennas and Propagation (InCAP)*, pp. 1–4, 2019. doi:10.1109/InCAP47789.2019.9134493
- [17] B. Mukherjee, P. Patel, and J. Mukherjee, "A review of the recent advances in dielectric resonator antennas," *Journal of Electromagnetic Waves and Applications*, vol. 34, no. 9, pp. 1095–1158, 2020. doi:10.1080/09205071.2020.1744484
- [18] A. Vahora, and K. Pandya, "Implementation of cylindrical dielectric resonator antenna array for Wi-Fi/wireless LAN/satellite applications," *Progress in Electromagnetics Research M*, vol. 90, pp. 157–66, 2020. doi:10.2528/PIERM20011604
- [19] R. Gupta, G. Bakshi, and A. Bansal, "Dual-band circularly polarized stacked sapphire and TMM13i rectangular DRA," *Progress In Electromagnetics Research M*, vol. 91, pp. 143–153, 2020. doi:10.2528/PIERM20012701
- [20] D. G. Patanvariya, A. Gaonkar, and S. Vardhan, "A Low Profile Modified Y-shaped RDRA for Triple-band Wireless Applications," *International Microwave and RF Conference (IMaRC)*, pp. 1–4, 2021. doi:10.1109/IMaRC49196.2021.9714687
- [21] M. Chauhan, A. Rajput, and B. Mukherjee, "Wideband circularly polarized low profile dielectric resonator antenna with meta superstrate for high gain," *AEU-International Journal of Electronics and Communications*, vol. 128, p.153524, 2021. doi:10.1016/j.aeue.2020.153524
- [22] CST GmbH. "CST Microwave Studio V.2018" [Online]. Available: <https://www.cst.com>
- [23] R. Xie, J. Cao, R. Wang, X. Wang, Z. Xu and S. Zhu, "A study of dielectric resonator antenna array applied to 5G communication system," *2016 Progress in Electromagnetic Research Symposium (PIERS)*, 2016, pp. 454–457, doi: 10.1109/PIERS.2016.7734363.